Journal of Organometallic Chemistry 755 (2014) 33–40

Contents lists available at ScienceDirect

Journal of Organometallic Chemistry

journal homepage: www.elsevier.com/locate/jorganchem

Synthesis and chemical–optical characterization of novel two-photon fluorescent borinates derived from Schiff bases

Cristina C. Jiménez [a], Norberto Farfán [a,*], Margarita Romero-Avila [a], Mario Rodríguez [b], Laura Aparicio-Ixta [b], Gabriel Ramos-Ortiz [b], José Luis Maldonado [b], Rosa Santillan [c], Nancy E. Magaña-Vergara [c], Ma. Eugenia Ochoa [c]

[a] Facultad de Química, Depto. de Química Orgánica, Universidad Nacional Autónoma de México, 04510 México D.F., Mexico
[b] Centro de Investigaciones en Óptica A.P. 1-948, 37000 León, Gto., Mexico
[c] Depto. de Química, Centro de Investigación y de Estudios Avanzados del IPN, Apdo. Postal. 14-740, 07000 México D.F., Mexico

ARTICLE INFO

Article history:
Received 10 January 2013
Received in revised form
11 December 2013
Accepted 21 December 2013

Keywords:
Borinates
Schiff bases
NLO properties
TPA or 2PA

ABSTRACT

Herein is reported the synthesis and characterization of eight borinates (**2a**–**h**) prepared from the reaction of the corresponding bidentate imine ligands (**1a**–**h**) and diphenylborinic acid. All compounds were characterized by MS, IR and NMR spectroscopies whereas the molecular structures of derivatives **2c** and **2e** were also studied by X-ray diffraction analysis that corroborated the presence of a tetra-coordinated boron atom. In addition, the linear and nonlinear optical (NLO) characterization of these molecules having D–π–C═N$^+$–π–D and D–π–C═N$^+$–π–A electronic systems was performed, i.e., the third-order nonlinear optical responses were measured by using the two-photon excited fluorescence and the third-harmonic generation (χ^3 determination) techniques. The borinates showed two-photon absorption (2PA) effect in solution under femtosecond excitation: **2g** and **2h** having D–π–C═N$^+$–π–A architecture showed the largest 2PA cross-sections (σ_{2PA}) values at 760 nm: 124 and 174 GM (1 GM = 10^{-50} cm^4 s), respectively, while the values for **2e** and **2f** that possess D–π–C═N$^+$–π–D structure were 12 and 37 GM. The χ^3 values, with nanosecond excitation, were of the order of 10^{-12} esu at 1200 nm.

1. Introduction

In the last two decades there has been an increasing interest in the study of materials possessing 2PA properties. In particular, great efforts have been devoted to develop organic chromophores with large 2PA cross-sections (σ_{2PA}) for a wide range of applications, which include up-converted lasing [1], data storage and microfabrication [2,3], two photon photodynamic therapy [4], labels to track the migration of non-fluorescent drugs inside the cells and for the localized release of bio-active species [5]. The research groups of Marder [6–8], Prasad [9], and Blanchard-Desce [10,11], are leading pioneers in this field.

For the design of 2PA chromophores, three essential components are required: a strong π-electron donor (D), a polarizable π-bridge, and a strong π-electron acceptor (A). Appropriate combinations and numbers of these components have resulted in molecular systems of three general classes: (i) dipolar, A–π–D (asymmetric); (ii) quadrupolar (symmetric), A–π–A, D–π–D, A–π–D–π–A, D–π–A–π–D; and (iii) octupolar; 3-branched, A_3–(D-core) and D_3–(A-core) [9]. For these systems the non-linear optical response is a non-trivial function of the donor and acceptor strengths, π-conjugated bridge length and type, nature of the conjugated core, torsional disorder, symmetry and topology [12]. Additionally, the opto-electronic properties can be tuned by the introduction into the π-plane of elements such as silicon [13], nitrogen [14], sulfur [15], phosphorus [16], and boron [17].

In the case of boron compounds their accessible structural design and facile synthesis [18] makes of them interesting materials for several photonic and opto-electronic devices [19], such as organic light-emitting diodes (OLEDs) [20,21], organic photovoltaic cells (OPVs) [22] and charge transport [23]. For these applications, the three coordinated boron species have received considerable attention since the vacant p-orbital is a strong π-electron acceptor, which promotes delocalization with adjacent organic conjugated systems and also these boron derivatives can function as sigma donor due to their electronegativity.

As for the four-coordinated systems, studies of the second-order NLO character have shown that this property is enhanced with

---

* Corresponding author.
E-mail address: norberto.farfan@gmail.com (N. Farfán).

0022-328X/$ – see front matter © 2014 Elsevier B.V. All rights reserved.
http://dx.doi.org/10.1016/j.jorganchem.2013.12.036

respect to the boron-free counterparts [24], as demonstrated in the case of theoretical [25–27] and experimental [24] studies of stilbazoles and pyridines. similarly, zwitterionic borates show much larger second-order NLO properties and higher transparency than the uncharged push–pull species [28,29]. Our research group has previously synthesized and optically characterized different boron complexes [30–33], studying the second- and the third-order optical nonlinearities in four-coordinated boron systems prepared from tridentate ligands. In this kind of compounds the appropriate combination of donor–acceptor groups and the formation of the N → B coordinative bond optimize the nonlinear optical effects. Among the advantages of tetra-coordinated compounds are an intrinsic high electron affinity, a large capacity to perturb the electronic structure by decreasing the LUMO level as well as the possibility to obtain very stable compounds with high transparency.

More recently, boron-containing two-photon absorbing fluorophores based on a pyrazabole [34] core have shown σ_{2PA} values of 325 GM around 800 nm; in particular, for the ferrocenyl substituted pyrazaboles, the two-photon absorption cross-section values were enhanced by increasing the conjugation giving values as high as 1016 GM [35]. Other boron-containing 2PA fluorophores are based on a one-dimensional conjugated system containing a terminal *p*-carborane unit and various donor groups at the other end. These systems exhibited 2PA cross-sections of 470 GM at 810 nm for the diphenylamino-substituted chromophore and 200–300 GM at 700 nm for the chromophores containing oxygen donor groups [36].

Investigations on the 2PA effect involving Schiff bases are scarce, in spite of their facile synthesis and design [37–42]. In general it has been shown that the cross section is highly increased upon complexation to metals. In particular, for boron derivatives of Schiff bases the studied systems include cyclodiborazane and pyrazabole moieties as central cores [43]. Following our research on boron complexes containing the coordinative N → B bond in electronic push–pull systems, and on the search for new fluorescent chromophores that could exhibit 2PA properties, we report herein the facile synthesis and characterization of eight strong fluorescent diphenylboron complexes (**2a**–**h**) with a strong electron donor group (–NEt$_2$) at the salicylidene derived fragment and different substituents at the aniline fragment. The aim of this study was to investigate the effect of the incorporation of different substituents as well as the influence of the boron atom on the fluorescent and NLO properties. Results show that while the Schiff bases exhibit poor fluorescence emission, after boron complexation, an intense green emission is observed when excited at 370 nm. Moreover, incorporation of electron withdrawing substituents at the aniline fragment of boron derived Schiff bases resulted in the enhancement of the third-order nonlinearities, i.e., 2PA effect and third-harmonic generation.

2. Experimental

2.1. Starting materials and equipment

Starting materials were commercially available and used without further purification. 4-Diethylaminobenzoate and 4-dimethylaminobenzoate were synthesized from 4-aminobenzoic acid using the method reported by Zheng [44] and compound **2b** was prepared as described in the literature [18]. Melting points were determined on a Fisher-Johns melting point apparatus and are uncorrected. Infrared spectra were obtained using a FT-IR (ATR) spectrophotometer. The ^{1}H, ^{11}B and ^{13}C NMR spectra were recorded on Jeol ECA 500, Varian Unity 300 and 400 MHz. Chemical shifts (ppm) are relative to $(CH_3)_4Si$ for ^{1}H and ^{13}C and $BF_3.Et_2O$ for ^{11}B, coupling constants are given in Hertz. Elemental analyses were obtained on an EA 1108 FISONS Instruments analyzer. MS spectra were obtained on a Thermo-Electron DFS (Double Focus Sector) with a double sector mass analyzer of inverse geometry. The high resolution mass spectra (HRMS) were determined with an Agilent spectro-photometer.

2.2. Crystal structure determination

Crystals of compounds **2c** and **2e** suitable for X-ray diffraction analysis were obtained by slow evaporation of solutions of chloroform:ethyl acetate at room temperature. Data collection was performed at 293 K on a Kappa CCD diffractometer with $\lambda_{\text{Mo-K}\alpha} = 0.71073$ Å radiation. The molecular structures of the compounds were solved by direct methods using SIR2004 [45] and were refined with SHELXL-97 [46], using full matrix least squares. All non-hydrogen atoms were refined anisotropically, the H atoms were refined using a riding model.

2.3. General procedure for the synthesis

The Schiff bases **1a**–**h** were obtained by reaction of equimolar amounts of 4-diethylamino-2-hydroxybenzaldehyde and the appropriate aniline under reflux of ethanol for 12 h. Solvent excess was eliminated with a Dean–Stark trap, the solid precipitated was collected by filtration and the products were purified by recrystallization technique from ethanol [47,48].

The series of borinates **2a**–**h** were prepared by reaction of the corresponding Schiff base and diphenylborinic acid obtained from the ethanol amine ester complex under reflux of ethyl acetate for 2 h. The borinates **2a**–**h** were obtained in good yields as yellow solids, which are soluble in common organic solvents.

2.3.1. *N,N-Diethyl-2,2,3-triphenyl-2H-benzo[e][1,3,2]oxazaborinin-7-amine (**2a**)*

The title compound was prepared from **1a** (0.50 g, 1.80 mmol) and 0.46 g (2.00 mmol) of diphenylborinic acid to give 0.44 g of **2a** in 55% yield. M.P: 165–167 °C. IR ν_{max}: 3069, 3040, 2974, 1612, 1585, 1507, 1352, 1267, 1237, 1205, 1188, 1137, 695 cm^{-1}. ^{1}H NMR ($CDCl_3$, 500 MHz) δ: 1.17 (6H, t, J = 7.1 Hz, $N(CH_2\underline{CH_3})_2$), 3.36 (4H, q, J = 7.1 Hz, $N(\underline{CH_2}CH_3)_2$), 6.15 (1H, s, H-2), 6.17 (1H, d, J = 2.2, Hz, H-4), 7.01–7.18 (12H, m, H-5, H-9, H-11, H-10, H-*m*, H-*p*), 7.44 (4H, d, J = 6.8 Hz, H-*o*), 8.08 (1H, s, H-7) ppm. ^{13}C NMR ($CDCl_3$, 75 MHz) δ: 12.8 (CH_3), 44.9 (CH_2), 98.7 (C-2), 105.2 (C-4), 109.5 (C-6), 124.5 (C-11), 126.0 (C-10), 126.9 (C*m*), 126.8 (C*p*), 128.6 (C-9), 134.0 (C*o*), 134.3 (C-5), 146.5 (C-8), 148.6 (C-*i*-B), 156.1 (C-3), 158.6 (C-7), 164.2 (C-1). MS (70 eV) m/z (%): 355 (M − 77, 100%), 311(30), 253(20), 432(2). HRMS calcd. m/z $C_{29}H_{30}BN_2O[M^+ + H]^+$: 433.2445 found: 433.2459. ^{11}B NMR ($CDCl_3$, 87 MHz) δ: 5.0 ppm. Anal. Calcd. C 80.56, H 6.76, N 6.48%. Found: C 80.50, N 6.93, H 6.49%.

2.3.2. *N,N-Diethyl-2,2-diphenyl-3(4-fluoro)-2H-benzo[e][1,3,2]oxazaborinin-7-amine (**2b**)*

N,N-Diethyl-2,2-diphenyl-3(4-fluoro)-2*H*-benzo[*e*][1,3,2]oxazaborinin-7-amine (**2b**) was prepared as described in the literature [18].

2.3.3. *N,N-Diethyl-2,2-diphenyl-3(4-chlorophenyl)-2H-benzo[e][1,3,2]oxazaborinin-7-amine (**2c**)*

The title compound was prepared from **1c** (0.56 g, 1.86 mmol) and 0.50 g, (2.20 mmol) of diphenylborinic acid to give 0.63 g of **2c** in 81% yield. M.P: 168–170 °C. IR ν_{max}: 3068, 3043, 2926, 2971, 1614, 1602, 1577, 1501, 1486, 1437, 1343, 1205, 1135, 1010, 882, 742, 698 cm^{-1}. ^{1}H NMR ($CDCl_3$, 300 MHz) δ: 1.18 (6H, t, J = 6.0 Hz, $N(CH_2\underline{CH_3})_2$), 3.37 (4H, q, J = 6.0 Hz, $N(\underline{CH_2}CH_3)_2$), 6.14 (1H, d,

$J = 3.0$ Hz, H-2), 6.18 (1H, dd, $J = 3.0, 9.0$ Hz, H-4), 7.07–7.23 (11H, m, H-5, H9, H-10, H-*m*, H-*p*), 7.44 (4H, dd, $J = 3.0, 9.0$ Hz, H-*o*), 8.04 (1H, s, H-7) ppm. ^{13}C NMR ($CDCl_3$, 75 MHz) δ: 12.7 (CH_3 NEt_2), 44.9 (CH_2 NEt_2), 98.6 (C-2), 105.3 (C-4), 109.3 (C-6), 125.5 (C-9), 126.0 (C-10), 126.9 (C-*m*), 128.5 (C-*p*), 132.3 (C-11), 133.7 (C-*o*), 134.2 (C-5), 144.9 (C-8), 148.4 (C-*i*), 156.3 (C-3), 158.2 (C-7), 164.2 (C-1), MS (70 eV) *m*/*z* (%): $[M^+ + H]^+$: 467 (3), 389 (M − 77, 100), 345 (35), HRMS calcd. *m*/*z* $C_{29}H_{29}BN_2OCl$ $[M^+ + H]^+$: 467.2055, found: 467.2067. ^{11}B NMR ($CDCl_3$, 96 MHz) δ: 5.5 ppm. Anal. Calcd. C 74.62, H 6.05, N, 6.00%. Found. C 74.15, H 5.59, N, 6.30%.

2.3.4. *N,N-Diethyl-2,2-diphenyl-3(4-iodophenyl)-2H-benzo[e][1,3,2]oxazaborinin-7-amine (**2d**)*

The title compound was prepared from **1d** (0.73 g, 1.86 mmol) and 0.50 g (2.20 mmol) of diphenylborinic acid to give 0.31 g of **2d** in 44% yield. M.P: 192–193 °C. IR ν_{max}3042, 3007, 2927, 2967, 1596, 1569, 1500, 1481, 1434, 1415, 1375, 1235, 1202, 1188, 1136, 975, 918, 794, 743, 701 cm^{-1}. ^{1}H NMR ($CDCl_3$, 400 MHz) δ: 1.16 (6H, t, $J = 8.0$ Hz, $N(CH_2\underline{CH_3})_2$), 3.35 (4H, q, $J = 8.0$ Hz, $N(\underline{CH_2}CH_3)_2$), 6.12 (1H, d, $J = 3.0$ Hz, H-2), 6.15 (1H, dd, $J = 9.0, 3.0$ Hz, H-4), 6.76 (2H, d, $J = 5.0$ Hz, H-9), 7.05 (1H, d, $J = 9.0$ Hz, H-5), 7.10–7.19 (6H, m, H-*m* H-*p*), 7.41–7.42 (6H, m, H-10, H-*o*), 8.01 (1H, s, H-7), ppm. ^{13}C NMR ($CDCl_3$, 75 MHz) δ: 12.7 (CH_3), 44.9 (CH_2), 91.5 (C-11), 98.5 (C-2), 105.4 (C-4), 109.4 (C-6), 126.0 (C-9), 126.1 (C-*p*), 126.8 (C-*m*), 133.7 (C-*o*), 134.2 (C-5), 137.4 (C-10), 146.0 (C-8), 148.0 (C-*i*), 156.3 (C-3), 158.0 (C-7), 164.0 (C-1), MS (70 eV) *m*/*z* (%): 558 (3) M^+, 482 (M^+ − 76, 24), 481 (100), 480 (24), 437 (15), 354 (17), 310 (15). HRMS calcd. *m*/*z* $C_{29}H_{29}BN_2OI[M^+ + H]^+$: 559.1411, found: 559.1405. ^{11}B NMR ($CDCl_3$, 87 MHz) δ: 5.5 ppm Anal. Calcd. C 62.39, N 5.02, H 5.06%. Found: C 62.16, N 5.22, H5.28%.

2.3.5. *N,N-Diethyl-2,2-diphenyl-3(4-methoxyphenyl)-2H-benzo[e][1,3,2]oxazaborinin-7-amine (**2e**)*

The title compound was prepared from **1e** (0.55 g, 1.86 mmol) and 0.50 g (2.20 mmol) of diphenylborinic acid to give 0.26 g, 33% yield of **2e**. M.P: 214–215 °C. IR ν_{max}: 3039, 2931, 2976, 1618, 1592, 1506, 1440, 1350, 1249, 1187, 1141, 1074, 1031, 835, 707 cm^{-1}. ^{1}H NMR ($CDCl_3$, 500 MHz) δ: 1.16 (6H, t, $J = 7.0$ Hz, $N(CH_2\underline{CH_3})_2$), 3.38 (4H, q, $J = 7.0$ Hz, $N(\underline{CH_2}CH_3)_2$), 3.68 (3H, s, OCH_3), 6.17 (1H, dd, $J = 9.0, 2.0$ Hz, H-4), 6.19 (1H, d, $J = 2.0$ Hz, H-2), 6.66 (2H, d, $J = 9.0$ Hz, H-10), 6.97 (2H, d, $J = 9.0$ Hz, H-9), 7.07 (1H, d, $J = 9.0$ Hz, H-5), 7.17 (2H, td, $J = 7.0, 2.0$ Hz, H-*p*), 7.23 (4H, td, $J = 7.0, 2.0$ Hz, H-*m*), 7.51 (4H, dd, $J = 7.0, 2.0$ Hz, H-*o*), 8.03 (1H, s, H-7) ppm. ^{13}C NMR ($CDCl_3$, 75 MHz) δ: 12.9 (CH_3), 45.0 (CH_2), 55.4 (OCH_3), 98.7 (C-2), 105.0 (C-4), 109.3 (C-6), 113.7 (C-10), 125.5 (C-9), 126.0 (C-*p*), 126.9 (C-*m*), 133.0 (C-*o*), 134.1 (C-5), 139.8 (C-8), 148.9 (C-3), 155.9 (C-11), 158.2 (C-7), 163.9 (C-1). MS (70 eV) *m*/*z* (%): 462 (4) M^+, 386 (30), 385 (M − 77, 100), 434 (30), 341 (42), 297 (25), 283 (18), 185 (42), 171 (22), 77 (18). HRMS calcd. *m*/*z* $C_{30}H_{32}BN_2O_2$ $[M^+ + H]^+$: 463.2551, found: 463.2563. ^{11}B NMR ($CDCl_3$, 87 MHz) δ: 4.8 ppm. Anal. Calcd. C 77.93, H 6.76, N 6.06%. Found. C 78.19, H 6.90, N 6.15%.

2.3.6. *N,N-Diethyl-2,2-diphenyl-3(4-diethylaminophenyl)-2H-benzo[e][1,3,2]oxazaborinin-7-amine (**2f**)*

The title compound was prepared from **1f** (0.63 g, 1.86 mmol) and 0.50 g (2.20 mmol) of diphenylborinic acid to give 0.31 g, 42% yield of **2f**. M.P: 183–184 °C. IR ν_{max}: 3067, 3045, 3002, 2867, 2973, 1608 (C=N), 1584, 1504, 1431, 1408, 1376, 1349, 1268, 1250, 1189, 1136, 1074, 1013, 971, 919, 898, 884, 744, 702 cm^{-1}. ^{1}H NMR ($CDCl_3$, 300 MHz) δ: 1.08 (6H, t, $J = 7.0$ Hz, $N(CH_2\underline{CH_3})_2$), 1.16 (6H, t, $J = 7.0$ Hz, $N(CH_2\underline{CH_3})_2$), 3.25 (4H, q, $J = 7.0$ Hz, $N(\underline{CH_2}CH_3)_2$), 3.35 (4H, q, $J = 7.0$ Hz, $N(\underline{CH_2}CH_3)_2$), 6.13 (1H, dd, $J = 8.0, 2.0$ Hz, H-4), 6.16 (1H, d, $J = 2.0$ Hz, H-2), 6.38 (2H, d, $J = 9.0$ Hz, H-10), 6.86 (2H, d, $J = 9.0$ Hz, H-9), 7.04 (1H, d, $J = 8.0$ Hz, H-5), 7.09–7.21 (6H, m, H-*m*, H-*p*), 7.47 (4H, dd, $J = 8.0, 2.0$ Hz, H-*o*), 8.02 (1H, s, H-7) ppm. ^{13}C NMR ($CDCl_3$, 75 MHz) δ: 12.5 (CH_3), 12.7 (CH_3), 44.3 (CH_2), 44.8 (CH_2), 98.7 (C-2), 104.5 (C-4), 109.3 (C-6), 110.9 (C-10), 125.1 (C-9), 125.7 (C-*p*), 126.8 (C-*m*), 133.5 (C-5), 133.8 (C-*o*), 135.1 (C-11), 146.5 (C-8), 155.3 (C-3), 156.9 (C-7), 163.4 (C-1) ppm. MS (70 eV) *m*/*z* (%): 503(M^+, 2), 426 (M^+ − 77, 100), 382 (17), 338 (8), 206 (11). HRMS calcd. *m*/*z* $C_{29}H_{29}BN_2OCl$ $[M^+ + H]^+$: 504.3180, found: 504.3185. ^{11}B NMR ($CDCl_3$, 87 MHz) δ: 4.8 ppm. Anal. Calcd. C 78.72, H 7.61, N 8.35%. Found: C 78.87, H 7.54, N 8.52%.

2.3.7. *N,N-Diethyl-2,2-diphenyl-3(4-methoxycarbonylphenyl)-2H-benzo[e][1,3,2]oxazaborinin-7-amine (**2g**)*

The title compound was prepared from **1g** (0.60 g, 1.86 mmol) and 0.50 g (2.20 mmol) of diphenylborinic acid to give 0.28 g of **2g** in 58% yield. M.P: 221–222 °C. IR ν_{max}: 3067, 3043, 3002, 2950, 2975, 1720 (C=O), 1619 (C=N), 1580, 1501, 1438, 1347, 1274, 1207, 1189, 1141, 1111, 1077, 972, 927, 742, 703 cm^{-1}. ^{1}H NMR ($CDCl_3$, 400 MHz) δ: 1.18 (6H, t, $J = 8.0$ Hz, $N(CH_2\underline{CH_3})_2$), 3.37 (4H, q, $J = 8.0$ Hz, $N(\underline{CH_2}CH_3)_2$), 3.84 (3H, s, OCH_3),6.13 (1H, d, $J = 4.0$ Hz, H-2), 6.18 (1H, dd, $J = 8.0, 2.0$ Hz, H-4),7.08–7.19 (9H, m, H-*m*, H-*p*, H-9, H-5),7.42 (4H, dd, $J = 8.0, 2.0$ Hz, H-*o*),7.79 (2H, d, $J = 9.0$ Hz, H-10), 8.10 (1H, s, NH) ppm. ^{13}C NMR ($CDCl_3$, 75 MHz) δ: 12.7 (CH_3), 45.0 (CH_2), 52.1 (OCH_3), 98.6 (C-2), 105.6 (C-4), 109.7 (C-6), 124.1 (C-9), 126.0 (C-*p*), 126.9 (C-*m*), 127.9 (C-11), 130.0 (C-10), 133.8 (C-*o*), 134.4 (C-5), 150.0 (C-8), 156.5 (C-3), 158.2 (C-7), 164.5 (C-1), 166.3 (CO) ppm. MS (70 eV) *m*/*z* (%): 490 (5) M^+, 489 (M^+ − 1, 10), 414 (26), 413 (M − 77, 100), 412 (20), 369 (25), 326 (20), 311 (45), 182 (20), 78 (42), 77 (15). HRMS calcd. *m*/*z* $C_{31}H_{32}BN_2O_3$ $[M^+ + H]^+$: 491.2500. Found: 491.2505. ^{11}B NMR ($CDCl_3$, 87 MHz) δ: 5.6 ppm. Anal. Calcd. C 75.92, H 6.37, N 5.71%. Found: C 76.56, H 6.42, N 5.79%.

2.3.8. *N,N-Diethyl-2,2-diphenyl-3(4-ethoxycarbonylphenyl)-2H-benzo[e][1,3,2] oxazaborinin-7-amine (**2h**)*

The title compound was prepared from **1h** (0.63 g, 1.86 mmol) and 0.50 g (2.20 mmol) of diphenylborinic acid to give 0.43 g, 58% yield of **2h**. M.P: 214–215 °C. IR ν_{max}: 3066, 3037, 3004, 2970, 1708 (C=O), 1616, (C=N), 1576, 1498, 1437, 1409, 1376, 1346, 1271, 1206, 1187, 1136, 1103, 1077, 971, 924, 884, 742, 702 cm^{-1}. ^{1}H NMR ($CDCl_3$, 500 MHz) δ: 1.18(6H, t, $J = 7.1$ Hz, $N(CH_2\underline{CH_3})_2$), 1.33 (3H, t, $J = 7.1$ Hz, $OCH_2\underline{CH_3}$), 3.36 (4H, q, $J = 7.1$ Hz, $N(\underline{CH_2}CH_3)_2$), 4.29 (2H, q, $J = 7.1$ Hz, OCH_2), 6.13 (1H, d, $J = 2.3$ Hz, H-2), 6.18 (1H, dd, $J = 2.4, 9.0$ Hz, H-4), 7.1–7.17 (9H, m, H-9, H-5, H-*m*, H-*p*), 7.44 (4H, dd, $J = 2.0, 8.0$ Hz, H-*o*), 7.80 (2H, d, $J = 8.0$ Hz H-10), 8.1 (1H, s, H-7) ppm. ^{13}C NMR ($CDCl_3$75 MHz) δ: 12.7 ($N{-}CH_2\underline{CH_3}$), 14.3 ($OCH_2\underline{CH_3}$), 45.0 (CH_2N), 61.0 (OCH_2), 98.5 (C-2), 105.6 (C-4), 109.7 (C-6), 124.0 (C-*p*), 126.0 (C-9), 126.9 (C-*m*), 128.3 (C-11), 129.9 (C-10), 133.8 (C-*o*), 134.5 (C-5), 148.2 (C-*i*), 150.0 (C-8), 156.5 (C-3), 158.2 (C-7), 164.5 (C-1), 165.8 (CO). MS (70 eV) *m*/*z* (%): 504 (2), 427 (M − 77, 100), 399 (15), 355 (17), 325 (14), 206 (7), 78 (12). HRMS calcd. *m*/*z* $C_{32}H_{34}BN_2O_3$ $[M^+ + H]^+$: 505.2657 Found: 505.2661. ^{11}B NMR ($CDCl_3$, 87 MHz) δ: 5.2 ppm. Anal. Calcd. C 76.19, H 6.59, N 5.55%. Found: C 76.24, H 6.18, N 5.79%.

2.4. *NLO measurements*

2.4.1. *Third-harmonic generation (THG) experiments*

Third-order NLO properties of borinates **2a–h** were first evaluated through the generation of visible optical frequencies in thin solid films when pumped with infrared optical frequencies. Thin films of each borinate were prepared in a guest:host approach using polystyrene as a host matrix doped with 30% of the guest. The films were deposited over glass substrates from chloroform solutions using the spin-coating method obtaining thicknesses in the range 250–265 nm. For optical setup information see previous work [31].

Briefly, the method consists in focusing infrared laser irradiation (1200 nm, pulses of 8 ns at a repetition rate of 10 Hz) into each tested film. The third-harmonic beam that emerges from films was selected by using a color filter and detected with a PMT and a lock-in amplifier. The THG measurements were performed for incident angles in the range from 40 to −40° with steps of 0.27° so that the nonlinear susceptibility $\chi^3(-3\omega, \omega, \omega, \omega)$ was calculated using the THG Maker-Fringes formalism [49–53].

2.4.2. Determination of quantum yields

Fluorescence quantum yield (Φ) for borinates **2a**–**h** were measured through the integration sphere method using Rhodamine 6G ($\Phi_{(ref)} = 0.95$) in methanol as a reference [54] and using a diode-laser (370 nm) as excitation source. The concentration of samples in THF solutions was 10^{-4} M. The Fluorescence quantum yield was estimated according to Eq. (1).

$$\Phi = \Phi_{(ref)} \frac{A_{(ref)}}{A} \frac{I}{I_{(ref)}} \tag{1}$$

where A and $A_{(ref)}$ are the absorption of sample and reference at the excitation wavelength, respectively, while I and $I_{(ref)}$ are the corresponding emission intensities.

2.4.3. Determination of 2PA cross-sections (σ_{2PA})

Two-photon excitation spectra for borinates **2a**–**h** in THF solution (1×10^{-4} M) were measured using the Two-Photon Excited Fluorescence technique (TPEF) [55,56] with a Ti:Sapphire laser (Spectra-Physics) as excitation source. The laser provided pulses of 100 fs with a repetition frequency of 80 MHz and was tunable in the wavelength range 740–830 nm. The laser radiation was focused inside a quartz cell (1 cm) by a focal lens (5 cm); to avoid absorption effects, the beam was focused close to the lateral cell wall. Then the fluorescent emission of the borinate solution was focused and recorded on a USB 4000, Ocean Optics spectrophotometer. The measurements were performed in an intensity regime where the fluorescence signal showed a quadratic dependence on the intensity of the excitation beam. A methanol solution of Rhodamine 6G (1×10^{-4} M), whose cross-sections values have been completely characterized in the literature [57,58], was employed as 2PA reference.

The 2PA cross-section of borinates was calculated at each wavelength according to Eq. (2), where C and n are the concentration and refraction index of the borinates and Rhodamine 6G solutions, while F is the integral of the TPEF spectrum.

$$\sigma_{2PA} = \sigma_{2PA(ref)} \frac{\Phi_{(ref)}}{\Phi} \frac{C_{(ref)}}{C} \frac{n_{(ref)}}{n} \frac{F}{F_{(ref)}} \tag{2}$$

In this equation the subindex *ref* stands for the solution Rhodamine 6G used as reference.

3. Results and discussion

The borinates **2a**–**h** were prepared from bidentate type Schiff bases. These borinates contain an electronic π-bridge that connects a strong donor group ($-NEt_2$) in one terminal of the molecular structure with a variety of substituents R_1 located at the other end (see Scheme 1). The R_1 substituents were selected to have different donating or accepting capabilities in order to form D–π–C=N$^+$–π–D and D–π–C=N$^+$–π–A systems.

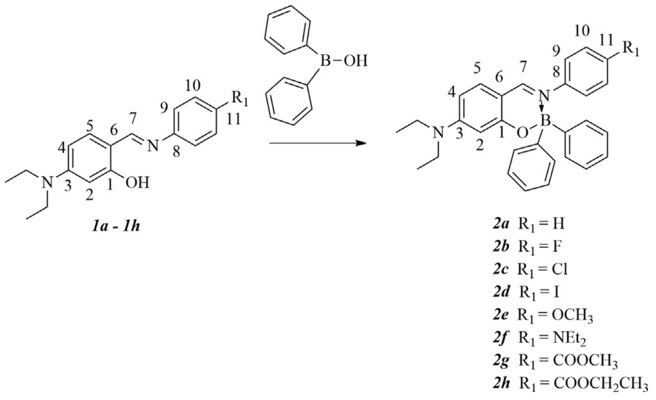

Scheme 1.

3.1. Spectroscopic characterization of the boron complexes 2a–h

The formation of borinates **2a**–**h** was evidenced by the shift of the C=N band (1596–1619 cm^{-1}) in the IR spectrum. In the ^{1}H NMR solution spectra, H-7 resonates from 8.01 to 8.44 ppm, this signal is shifted to low frequency with respect to the corresponding Schiff base. The imine carbon appears from 156.9 to 159.9 ppm in the ^{13}C NMR spectra, in agreement with previous reports [32,33]. The presence of four-coordinated boron atoms in **2a**–**h** was confirmed by the ^{11}B NMR signal from 4.8 to 5.6 ppm.

3.2. Crystal structure of borinates

Suitable crystals for compounds **2c** and **2e** were obtained from saturated solutions by slow evaporation of the solvent at room temperature. The most relevant crystallographic parameters are given in Table 1. Compound **2c** crystallized into the monoclinic system with space group $P2_1/c$ containing two borinate molecules and a molecule of ethyl acetate (solvent) per asymmetric unit and four molecules per unit cell Fig. 1. While compound **2e** crystallized in the triclinic system with space group P−1 containing two borinate molecules per unit cell Fig. 2.

The X-ray diffraction data from compounds **2c** and **2e** corroborate the presence of a tetra-coordinated boron atom, the angles around this atom (from 105.3(3) to 109.3(3)° for **2c** and from

Table 1
Selected crystal and refinement data for compounds **2c** and **2e**.

	2c	**2e**
Formula	$2(C_{29}H_{28}BClN_2O)\cdot C_4H_8O_2$	$C_{30}H_{31}BN_2O_2$
MW/g mol^{-1}	1021.69	462.38
Crystal system	Monoclinic	Triclinic
Space group	$P2_1/c$	P-1
a/Å	11.5250 (1)	10.5920 (2)
b/Å	41.8790 (5)	11.2214 (2)
c/Å	12.1040 (2)	12.7019 (3)
α (°)	90.0	70.0883 (8)
β (°)	105.340 (1)	87.8000 (8)
γ (°)	90.0	63.2112 (9)
V/Å^3	5633.93 (12)	1255.14 (5)
Z	4	2
ρ_c/g cm^{-3}	1.20	1.22
Collected Refl.	22,957	17,993
Ind. Ref. (Rint)	11,357(0.046)	5663(0.034)
Observed Ref	4665	4168
$R[F^2 > 2\sigma(F^2)]$	0.062	0.051
R_w (all data)	0.235	0.174
$\Delta\rho_{max}$/e Å^3	0.46	0.273
$\Delta\rho_{min}$/e Å^3	−0.48	−0.325

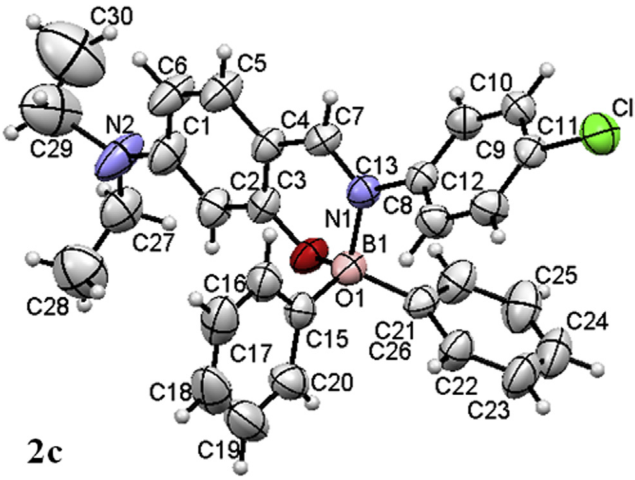

Fig. 1. Molecular structure of compound **2c** with displacement ellipsoids drawn at the 35% probability level.

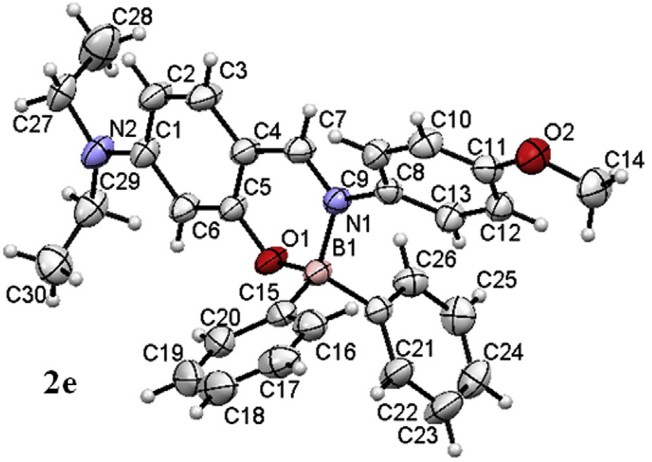

Fig. 2. Molecular structure of compounds **2e** with displacement ellipsoids drawn at the 35% probability level.

103.60(12) to 114.37(12)° in **2e**) are closed to tetrahedral angle values. The N → B bond lengths for compounds **2c** and **2e** are: 1.630 (5) Å and 1.631 (2) Å, respectively, these data are in agreement with values previously reported for analogous compounds where these bond distances are between 1.602(3) Å and 1.646(3) Å [32–34]. A summary of bond length distances and angles around de boron atom are shown in Table 2 and Table 3. A non-planar conformation on the main π-backbone of the borinates is observed from the torsion angles values for the fragment C(7)–N(1)–C(8)–C(9), resulting in −48.0(4)° for **2c** and 39.93(19)° for **2e**, which are similar to those previously reported [18,31].

Table 2
Selected bond lengths [Å].

	2c	2e
C21–B1	1.605 (5)	1.622 (2)
C15–B1	1.608 (6)	1.622 (2)
B1–O1	1.516 (4)	1.5061 (19)
B1–N1	1.630 (5)	1.631 (2)
C7–N1	1.310 (4)	1.3115 (18)
C21A–B1A	1.615 (5)	
C15A–B1A	1.616 (5)	
B1A–O1A	1.517 (4)	
B1A–N1A	1.613 (5)	

Table 3
Selected angles [°] around the boron atom.

	2c	2e
O1–B1–C_{ph}	109.1 (3)	110.45 (13)
O1–B1–C_{ph}	107.3 (3)	103.60 (12)
C15–B1–C21	117.2 (3)	114.37 (12)
O1–B1–N1	105.3 (3)	106.88 (11)
C_{ph}–B1–N1	109.3 (3)	107.93 (12)
C_{ph}–B1–N1	107.9 (3)	113.32 (12)
C9–C8–N1–C7	−48.0 (4)	39.93 (19)
O1A–B1A–C15A	107.4 (3)	
O1A–B1A–C21A	110.6 (3)	
C15A–B1A–C21A	115.1 (3)	
O1A–B1A–N1A	104.4 (3)	
C15A–B1A–N1A	109.5 (3)	
C21A–B1A–N1A	109.2 (3)	
C9A–C8A–N1A–C7A	−60.1 (5)	

Table 4
Photophysical properties of borinates **2a–h**.

Molecule	λ_{abs} (nm)	$\varepsilon \times 10^3$ (L cm^{-1} mol^{-1})	λ_{em} (nm)	Φ[a]	σ_{2PA} (GM)[b]
2a	402	42	502	0.11	53
2b	402	39	494	0.11	49
2c	409	48	500	0.16	85
2d	417	38	503	0.17	100
2e	403	37	513	0.03	37
2f	425	38	547	0.04	12
2g	418	55	503	0.10	124
2h	425	46	504	0.26	174

[a] Using Rhodamine 6G as reference, $\Phi = 0.95$ in methanol, $\lambda_{ex} = 370$ nm.
[b] Using excitation at 760 nm.

A detailed examination of the supramolecular structure for compounds **2c** and **2e** shows that the crystalline arrangement is governed by CH–π interactions due to the absence of co-planarity between the phenyl rings, where the CH groups act as donors. For compound **2c**, this interaction is described by the C2–H2···centroid 1 (C15–C20) with a distance of 3.675 Å and the angle is 151° with symmetry code [2575] = −*x*, 2 − *y*, −*z*. The crystal structure has an intramolecular hydrogen bond formed by the interactions of C(20)–H(20)···O(1) [$d_{O1\cdots C20} = 2.878(3)$ Å]. See Supplementary material.

The supramolecular structure of compound **2e** shows several CH–π interactions (see Supplementary material), one of these involves the C12–H12···centroid 7 (C15A–C20A) with a distance of 3.720(4) Å, an angle of 140° and symmetry code [1555] = *x*, *y*, *z*. Another intramolecular interaction is that of C17A–H17A···centroid 3 (C15–C20) with a distance of 3.805(5) Å, an angle of 152° and with symmetry code [1555] = *x*, *y*, *z*. Additionally, the crystal structure of compound **2c** shows an intermolecular hydrogen bond between the C7–H7···O3 interaction) [$d_{O3\cdots C7} = 3.423(6)$ Å] with symmetry code [3556] = −*x*, −*y*, 1 − *z*. Other important intramolecular hydrogen bonds are formed by the interaction of C(16)–H(16)···N1 [$d_{O1\cdots C20} = 2.878(3)$ Å], C(16A)–H(16A)···O(1A) [$d_{O1A\cdots C16A} = 2.865(4)$ Å], and C(16A)–H(16A)···O(1A) [$d_{O1A\cdots C16A} = 2.865(4)$ Å.

3.3. Optical characterization

3.3.1. Lineal absorption and light emission

The photophysical properties of borinates **2a–h** are summarized in Table 4. The linear absorption and emission spectra for the boron complexes in THF solution are shown in Fig. 3. These boron complexes have an intense absorption band from 402 to 425 nm, which is assigned to typical $n \rightarrow \pi^*$ electronic transition. In particular, compounds **2g** and **2h** possessing both the strong donor (−NEt$_2$) but different acceptor groups (−COOEt and −COOMe), showed a red shift $\Delta\lambda$ of 16 and 23 nm, respectively, compared with the absorption band of the borinate **2a** (having a −H end group). Similarly, a shift of 23 nm was observed in the case of compound **2f** containing the −NEt$_2$ donor group in a quadrupolar architecture D−π−C=N$^+$−π−D. In the case of borinate **2e**, possessing a quadrupolar architecture with an −OMe group, the absorption band is similar to **2a**. It is also observed an increment of molar absorption (ε) in compounds with architecture D−C=N$^+$−A and surprisingly a reduction in compounds with D−C=N$^+$−D design.

It is important to note that, after boron complexation, compounds **2a**−**h** give intense green emission (band around 500 nm) when excited at 370 nm. Compound **2f**, possessing a D−π−C=N$^+$−π−D architecture (with −NEt$_2$ as donor groups) showed the largest Stoke shift (81,967 cm^{-1}) of this series of borinates, while compound **2e** containing the combination of −NEt$_2$ and −OMe groups connected to the main π−backbone, has also a considerable Stoke shift (90,909 cm^{-1}). However, compounds **2h** and **2g** with D−π−C=N$^+$−π−A architectures with −COOEt and −COOMe acceptor groups showed larger Stoke shifts of 117,647 cm^{-1} and 126,582 cm^{-1}, respectively. Quantum yields Φ for all borinates were measured in THF solutions, giving values from 0.03 to 0.26 (see Table 4), which are in agreement with those values obtained from similar boron compounds (0.01−0.6) reported by other authors [18]. But lower that those reported in the range 0.31−0.65 for boron compounds derivates from benzoxazole [59]. A possible explanation of the low Φ values is the non-planar conformation observed in the π-backbone of **2c** and **2e** (see X-ray diffraction analysis section) in comparison to the π-system of benzoxazole derivatives that have flat conformation. In general, the experimental Φ values obtained from **2a**−**h** showed a dramatic decrement for compounds with D−C=N$^+$−D architecture, in which there is an increase of electronic density in the π-skeleton.

3.3.2. *Non-linear optical characterization*

The third-order nonlinear susceptibility (χ^3) for the series **1a**−**h** and **2a**−**h** was first evaluated at the telecommunication wavelength of 1200 nm by THG Maker-fringes technique. THG signal (400 nm) was measured for the polymeric film doped with ligands **1a**−**h** or borinates **2a**−**h**. The level of THG signal from ligands **1a**−**h** and borinates **2b** and **2d**−**g** was very weak and below the sensibility of our experimental setup. However, polymeric films doped with borinates **2a**, **2c** and **2h** generated significant THG signals. The plots of THG as a function of the angle of incidence for the fundamental beam were used to apply THG-Marker formalism. The so obtained values of χ^3 were 1.82, 1.48 and 2.28 × 10^{-12} esu for **2a**, **2c** and **2h**, respectively. These values are slightly larger than those recorded for borinates (1.1−1.5 × 10^{-12} esu) containing D−π−A architecture, with strong acceptor −NO$_2$ groups reported previously [31].

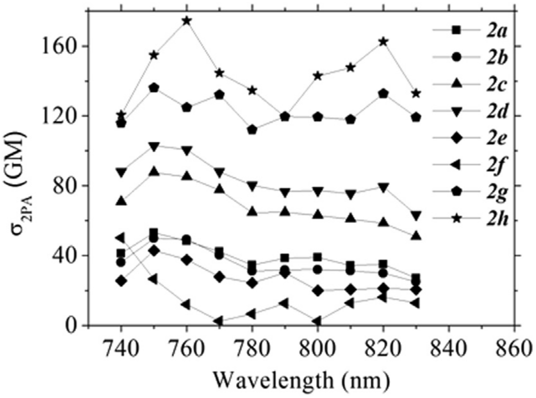

Fig. 4. 2PA cross section spectra of borinates **2a**−**h** in THF solution.

Note that these values of χ^3 were obtained at 1200 nm, which is exactly 3 times the wavelength where the maximum linear absorption of the boron compounds is located. Despite the possible presence of resonant effects, the THG technique was employed since it is a quick screening method to evaluate the nonlinearities, and in our case permitted to determine easily that **2h** (with the architecture D−π−C=N$^+$−π−A) exhibited the most efficient nonlinear response in the molecular series studied herein. This was also proved through a different nonlinear optical effect, i.e., 2PA performed in another region of wavelengths (see discussion below).

3.3.3. *Two-photon absorption properties of borinates **2a**−**h***

To obtain information of the efficiency of the 2PA process in this series of compounds, the cross section (σ_{2PA}) of borinates **2a**−**h** were calculated from data of TPEF experiments. This technique is based on a comparison of the two-photon excited fluorescence spectra from the sample (borinate) with a standard (Rhodamine 6G). Fig. 4 displays the values measured for σ_{TPA} at the wavelength range 740−830 nm. From this figure we observe that at such wavelength range the molecules exhibit only small variations in their σ_{2PA} values. For shorter wavelengths (corresponding to energies higher than the one-photon transitions that define the peaks shown in Fig. 3a), it is expected that some 2PA resonances might occur. In our case, however, the two-photon absorption spectra were not extended to shorter wavelengths due to the limited tunability of our laser system. Nevertheless, the σ_{TPA} values shown

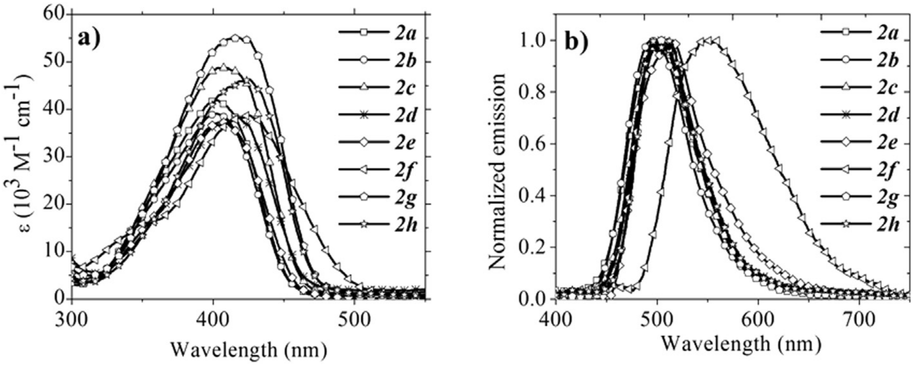

Fig. 3. Linear absorption a) and emission b) spectra for borinates **2a**−**h** in THF.

in Fig. 4 allowed comparison of the effect of the molecular structure on the nonlinear optical properties.

The studied borinates can be grouped in two categories, those comprising a $D{-}\pi{-}C{=}N^{+}{-}\pi{-}D$ architecture with strong electron donor groups at the end of the molecule, i.e., **2e** ($-OCH_3$) and **2f** ($-NEt_2$), and compounds containing a $D{-}\pi{-}C{=}N^{+}{-}\pi{-}A$ architecture, **2b** ($-F$), **2c** ($-Cl$), **2d** ($-I$), **2g** ($-COOCH_3$) and **2h** ($-COOCH_2CH_3$). Surprisingly, the architecture $D{-}\pi{-}C{=}N^{+}{-}\pi{-}D$ produced the lowest values of σ_{2PA} and the smallest fluorescence quantum yields. Larger values of σ_{2PA} were obtained for the $D{-}\pi{-}C{=}N^{+}{-}\pi{-}A$ architecture, and for the particular case of **2b**, **2c**, and **2d** the cross section values are inversely related to the electronegativity. For the same architecture, the highest cross section was found for the ester groups **2g** and **2h** where the acceptor provides stabilization. Notice that there is an agreement between the 2PA and THG experiments, in both cases the most significant optical nonlinearities were observed for **2h**. This molecular system also exhibited the largest fluorescence quantum yield among all set of studied molecules.

The values of Φ and σ_{2PA} observed around 800 nm for **2h** are very similar to those observed in pyrazabole based fluorescent bioprobes [34], although somewhat smaller (about half the value) compared with boron-containing two-photon-absorbing fluorophores based on the *p*-carborane entity [36], however, it must be recognized that in the latter case a more complex synthetic procedure is required. Indeed, our borinates derived from Schiff bases comprise a simple synthesis process. The system **2h** with architecture $D{-}\pi{-}C{=}N^{+}{-}\pi{-}A$ has larger two-photon activity (light emission induced by 2PA) than ferrocenyl substituted pyrazaboles with architecture $D{-}\pi{-}A{-}\pi{-}D$ [35]. The substituted pyrazaboles exhibit σ_{2PA} values of the order of 10^3 GM, but it was not reported if they can emit light induced by 2PA. Furthermore, their relatively large σ_{2PA} was measured by Z-scan technique with nanosecond pulses at 532 nm, but such long temporal pulses induce multi-step nonlinear absorption, while in the case of our borinates the σ_{2PA} values is due exclusively to simultaneous absorption of two photons.

4. Conclusions

Novel borinates were conveniently synthesized from the reaction of diphenylborinic acid and bidentate ligands. After complexation of these ligands, all of the borinates exhibit fluorescence induced by absorption of one- or two-photons at the wavelengths about 400 and 800 nm, respectively. Likewise, the third-order nonlinearities of such borinates were notoriously enhanced in comparison with their corresponding ligands. The highest two-photon absorption cross-section ($\sigma_{TPA} = 174$ GM) of the series of studied compounds corresponds to **2h** with a $D{-}\pi{-}C{=}N^{+}{-}\pi{-}A$ ($D = NEt_2$ and $A = COOCH_2CH_3$) architecture. The borinate **2f**, with a $D{-}\pi{-}C{=}N^{+}{-}\pi{-}D$ architecture ($D = NEt_2$), has the lowest value (12 GM). In the case of borinates **2b**, **2c** and **2d**, the cross section is inversely related to the electronegativity of the halogenated compounds, decreasing in the following order **2b** (F) < **2c** (Cl) < **2d** (I). The low cross-sections values for borinates **2c** (85 GM) and **2e** (37 GM) could be attributed to the structural deformation after boron complexation on the main π-backbone, confirmed by the X-ray diffraction analysis. Compounds **2a**–**h** are derivatives of Schiff bases that comprise facile design and synthesis at low cost.

Acknowledgements

Authors thank CONACyT-CNRS-LIA and PAPIIT (Grant IN-214513) for financial support. Gabriel Ramos-Ortiz thanks CONACyT (Grant 132946). Cristina C. Jiménez thanks CONACyT for a Ph.D. Fellowship (167206) and Nancy E. Magaña-Vergara thanks ICyT.

Appendix A. Supplementary material

CCDC Nos. 914469 and 914470 contain the supplementary crystallographic data for this paper. These data can be obtained free of charge from The Cambridge Crystallographic Data Centre via www.ccdc.cam.ac.uk/data_request/cif.

Appendix B. Supplementary data

Supplementary data related to this article can be found at http://dx.doi.org/10.1016/j.jorganchem.2013.12.036.

References

[1] T.-C. Lin, S.-J. Chung, K.-S. Kim, X. Wang, G.-S. He, J. Swiatkiewicz, H.E. Pudavar, P.N. Prasad, Adv. Polym. Sci. 161 (2003) 157–193.
[2] C.N. LaFratta, J.T. Fourkas, T. Baldacchini, R.A. Farrer, Angew. Chem. Int. Ed. 46 (2007) 6238–6258.
[3] B.H. Cumpston, S.P. Ananthavel, S. Barlow, D.L. Dyer, J.E. Ehrlich, L.L. Erskine, A.A. Heikal, S.M. Kuebler, I.-Y.S. Lee, D. McCord-Maughon, J.Q. Qin, H. Röckel, M. Rumi, X.-L. Wu, S.R. Marder, J.W. Perry, Nature 398 (1999) 51–54.
[4] N. Adarsh, R.R. Avirah, D. Ramaiah, Org. Lett. 12 (2010) 5720–5723.
[5] L. Hunyady, A.J. Baukal, Z. Gáborik, J.A. Olivares-Reyes, M. Bor, M. Szaszák, R. Lodge, K.J. Catt, T. Balla, J. Cell. Biol. 157 (2002) 1211–1222.
[6] L. Beverina, J. Fu, A. Leclercq, E. Zojer, P. Pacher, S. Barlow, E.W. Van Stryland, D.J. Hagan, J.L. Brédas, S.R. Marder, J. Am. Chem. Soc. 127 (2005) 7282–7283.
[7] S.J.K. Pond, M. Rumi, M.D. Levin, T.C. Parker, D. Beljonne, M.W. Day, J.-L. Brédas, S.R. Marder, J.W. Perry, J. Phys. Chem. A 106 (2002) 11470–11480.
[8] S.-J. Chung, S. Zheng, T. Odani, L. Beverina, J. Fu, L.A. Padilha, A. Biesso, J.M. Hales, X. Zhan, K. Schmidt, A. Ye, E. Zojer, S. Barlow, D.J. Hagan, E.W. Van Stryland, Y. Ying, Z. Shuai, G.A. Pagani, J.-L. Brédas, J.W. Perry, S.R. Marder, J. Am. Chem. Soc. 128 (2006) 14444–14445.
[9] G.S. He, L.-S. Tan, Q. Zheng, P.N. Prasad, Chem. Rev. 108 (2008) 1245–1330.
[10] C. Katan, S. Tretiak, M.H.V. Werts, A.J. Bain, R.J. Marsh, N. Leonczek, N. Nicolaou, E. Badaeva, O. Mongin, M. Blanchard-Desce, J. Phys. Chem. B 111 (2007) 9468–9483.
[11] F. Terenziani, C. Katan, E. Badaeva, S. Tretiak, M. Blanchard-Desce, Adv. Mater. 20 (2008) 4641–4678.
[12] M. Charlot, N. Izard, O. Monguin, D. Riehl, M. Blanchard-Desce, Chem. Phys. Lett. 417 (2006) 297–302.
[13] T. Wang, A.J. Pearson, D.G. Lidzey, J. Mater. Chem. C 1 (2013) 7266–7293.
[14] D.-J. Liawa, K.-L. Wang, Y.-C. Huanga, K.-R. Lee, J.-Y. Lai, C.-S. Ha, Prog. Polym. Sci. 37 (2012) 907–974.
[15] C.-H. Tsai, D.N. Chirdon, A.B. Maurer, S. Bernhard, K.J.T. Noonan, Org. Lett. 15 (2013) 5230–5233.
[16] T. Baumgartner, R. Réau, Chem. Rev. 106 (2006) 4681–4727.
[17] X. He, T. Baumgartner, RSC Adv. 3 (2013) 11334–11350.
[18] D. Frath, S. Azizi, G. Ulrich, P. Retailleau, R. Ziessel, Org. Lett. 13 (2011) 3414–3417.
[19] D. Li, Z. Zhang, S. Zhao, Y. Wang, H. Zhang, Dalton Trans. 40 (2011) 1279–1285.
[20] L. Xiao, Z. Chen, B. Qu, J. Luo, S. Kong, Q. Gong, J. Kido, Adv. Mater. 23 (2011) 926–952.
[21] F. Jäkle, Chem. Rev. 110 (2010) 3985–4022.
[22] A. Mishra, P. Bäuerle, Angew. Chem. Int. Ed. 51 (2012) 2020–2067.
[23] A. Wakamiya, T. Taniguchi, S. Yamaguchi, Angew. Chem. Int. Ed. 45 (2006) 3170–3173.
[24] M.J.G. Lesley, A. Woodward, N.J. Taylor, T.B. Marder, I. Cazenobe, I. Ledoux, J. Zyss, A. Thornton, D.W. Bruce, A.K. Kakkar, Chem. Mater. 10 (1998) 1355–1365.
[25] Rajneesh Misra, Thaksen Jadhav, Shaikh M. Mobin, Dalton Trans. 43 (2014) 2013–2022.
[26] D. Locatelli, S. Quici, D. Roberto, F. De Angelis, Chem. Commun. (2005) 5405–5407.
[27] Z.M. Su, X.J. Wang, Z.H. Huang, R.S. Wang, J.K. Feng, J.Z. Sun, Synth. Met. 119 (2001) 583–584.
[28] C. Lambert, S. Stadler, G. Bourhill, C. Bräuchle, Angew. Chem. Int. Ed. 35 (1996) 644–646.
[29] C.D. Entwistle, T.B. Marder, Angew. Chem. Int. Ed. 41 (2002) 2927–2931.
[30] H. Reyes, B.M. Muñoz, N. Farfán, R. Santillan, S. Rojas-Lima, P.G. Lacroix, K. Nakatani, J. Mater. Chem. 12 (2002) 2898–2903.
[31] M. Rodríguez, J.L. Maldonado, G. Ramos-Ortíz, O. Domínguez, Ma. E. Ochoa, R. Santillan, M.A. Meneses-Nava, O. Barbosa-García, Polyhedron 43 (2012) 194–200.
[32] M. Rodríguez, J.L. Maldonado, G. Ramos-Ortíz, J.L. Lamère, P.G. Lacroix, N. Farfán, Ma. E. Ochoa, R. Santillan, M.A. Meneses-Nava, O. Barbosa-García, K. Nakatani, New J. Chem. 33 (2009) 1693–1702.
[33] M. Rodríguez, R. Castro-Beltrán, G. Ramos-Ortíz, J.L. Maldonado, N. Farfán, O. Domínguez, J. Rodríguez, R. Santillan, M.A. Meneses-Nava, O. Barbosa-García, J. Peon, Synth. Met. 159 (2009) 1281–1287.

[34] A. Hayek, F. Bolze, C. Bourgogne, P.L. Baldeck, P. Didier, Y. Arntz, Y. Mely, J.-F. Nicoud, Inorg. Chem. 48 (2009) 9112–9119.

[35] T. Jadhav, R. Maragani, R. Misra, V. Sreeramulu, D. Narayana Rao, S.M. Mobin, Dalton Trans. 42 (2013) 4340–4342.

[36] J.F. Nicoud, F. Bolze, X.H. Sun, A. Hayek, P. Baldeck, Inorg. Chem. 50 (2011) 4272–4278.

[37] A. Jana, S.Y. Jang, J.-Y. Shin, A.K. De, D. Goswami, D. Kim, P.K. Bharadwaj, Chem. Eur. J. 14 (2008) 10628–10638.

[38] J.S. Zugazagoitia, M. Maya, C. Damián-Zea, P. Navarro, H.I. Beltrán, J. Peon, J. Phys. Chem. A 114 (2010) 704–714.

[39] L. Tian, Z. Hu, P. Shi, H. Zhou, J. Wu, Y. Tian, Y. Zhou, X. Tao, M. Jiang, J. Lumin. 127 (2007) 423–430.

[40] J. Zhanga, C. Zhong, X. Zhub, H.-L. Tam, K.-F. Li, K.-W. Cheah, W.-Y. Wong, W.-K. Wong, R.A. Jones, Polyhedron 49 (2013) 121–128.

[41] Z. Ye, L. De Boni, U.M. Neves, C.R. Mendonça, X.R. Bu, Tetrahedron Lett. 50 (2009) 1371–1373.

[42] M.-L. Zhang, Y.-P. Tian, X.-J. Zhang, J.-Y. Wu, S.-Y. Zhang, D. Wang, M.-H. Jiang, S. Chantrapromm, H.-K. Fun, Trans. Met. Chem. 29 (2004) 596–602.

[43] F. Bolze, A. Hayek, X.H. Sun, P.L. Baldeck, C. Bourgogne, J.-F. Nicoud, Opt. Mater. 33 (2011) 1453–1458.

[44] Q.-Z. Zheng, F. Zhang, K. Cheng, Y. Yang, Y. Chen, Y. Qian, H.-J. Zhang, H.-Q. Li, C.-F. Zhou, S.-Q. An, Q.-C. Jiao, H.-L. Zhu, Bioorg. Med. Chem. 18 (2010) 880–886.

[45] M.C. Burla, R. Caliandro, M. Camalli, B. Carrozzini, G.L. Cascarano, L. De Caro, C. Giacovazzo, G. Polidori, R. Spagna, J. Appl. Crystallogr. 38 (2005) 381–388.

[46] G.M. Sheldrick, SHELXL-97, Program for Refinement of Crystal Structures, University of Göttingen, Göttingen, Germany, 1996.

[47] G.P. Moloney, R.W. Gable, M.N. Iskander, D.J. Craik, M.F. Mackay, Aust. J. Chem. 43 (1990) 99–107.

[48] J.P. Raval, K.R. Desai, Chemija 20 (2009) 101–108.

[49] P.D. Maker, R.W. Terhune, M. Nisenoff, C.M. Savage, Phys. Rev. Lett. 8 (1962) 21–22.

[50] J. Jerphagnon, S.K. Kurtz, J. Appl. Phys. 41 (1970) 1667–1681.

[51] G.R. Meredith, Phys. Rev. B 24 (1981) 5522–5532.

[52] F. Kajzar, J. Messier, C. Rosilio, J. Appl. Phys. 60 (1986) 3040–3044.

[53] X.H. Wang, D.P. West, N.B. McKeown, T.A. King, J. Opt. Soc. Am. B 15 (1998) 1895–1903.

[54] N.S. Makarov, M. Drobizhev, A. Rebane, Opt. Exp. 16 (2008) 4029–4047.

[55] H.M. Kim, B.R. Cho, Chem. Commun. (2009) 153–164.

[56] M. Pawlicki, H.A. Collins, R.G. Denning, H.L. Anderson, Angew. Chem. Int. Ed. 48 (2009) 3244–3266.

[57] C. Xu, W.W. Webb, J. Opt. Soc. Am. B 13 (1996) 481–491.

[58] A. Fischer, C. Cremer, E.H.K. Stelzer, Appl. Opt. 34 (1995) 1989–2003.

[59] D. Li, H. Zhang, C. Wang, S. Huang, J. Guo, Y. Wang, J. Mater. Chem. 22 (2012) 4319–4328.